Equid que venihi tasped volut officillum sidit lam p. XX

Human gut commensals produce diverse genotoxins pp. 358 & 369

Martian meteorite impact pp. 360, 412, & 417

Science

$15
28 OCTOBER 2022
science.org

AAAS

BIG CHANGE

Mammalian skull evolution rates vary across taxa

pp. 355 & 377

MAMMALIAN EVOLUTION

Attenuated evolution of mammals through the Cenozoic

Anjali Goswami[1,2]*, Eve Noirault[1], Ellen J. Coombs[1,2,3], Julien Clavel[4], Anne-Claire Fabre [1,5,6], Thomas J. D. Halliday[1,7], Morgan Churchill[8], Abigail Curtis[9], Akinobu Watanabe[1,10,11], Nancy B. Simmons[12], Brian L. Beatty[10,13], Jonathan H. Geisler[10,13], David L. Fox[14], Ryan N. Felice[1,2,15]

The Cenozoic diversification of placental mammals is the archetypal adaptive radiation. Yet, discrepancies between molecular divergence estimates and the fossil record fuel ongoing debate around the timing, tempo, and drivers of this radiation. Analysis of a three-dimensional skull dataset for living and extinct placental mammals demonstrates that evolutionary rates peak early and attenuate quickly. This long-term decline in tempo is punctuated by bursts of innovation that decreased in amplitude over the past 66 million years. Social, precocial, aquatic, and herbivorous species evolve fastest, especially whales, elephants, sirenians, and extinct ungulates. Slow rates in rodents and bats indicate dissociation of taxonomic and morphological diversification. Frustratingly, highly similar ancestral shape estimates for placental mammal superorders suggest that their earliest representatives may continue to elude unequivocal identification.

Placental mammals make up 94% of extant mammalian diversity, with more than 6100 recognized extant species (*1*). This richness in species numbers is paired with an immense variation in ecology and morphology, with fully volant to fully aquatic forms spanning six orders of magnitude in size. Much diversification of placental mammals is thought to have been achieved quickly in the early Cenozoic, in the aftermath of the Cretaceous-Paleogene (K/Pg) mass extinction that removed nonavian dinosaurs from global ecosystems (*2*). However, despite a wealth of data from extant and fossil species, the timing, tempo, and drivers of the placental mammal morphological radiation have remained contentious. Studies of body size evolution variably support an early burst (*3*), accelerating rates linked to climate (*4*), or stable rates after the initial superordinal divergences. These studies often suggest that the K/Pg event had little impact on placental mammal evolution (*5*). By contrast, studies of tooth morphology or discrete character data suggest that either morphological diversification postdated the K/Pg extinction (*6*, *7*) or that rates of evolution increased rapidly at K/Pg boundary (*8*). Some of this uncertainty is due to the ongoing debate on the timing of origin of Placentalia and its proximity to the K/Pg mass extinction (*9*–*16*). Two additional critical factors contribute to this uncertainty: (i) the exclusion of fossils from most studies, despite wholly extinct lineages dominating the initial post-K/Pg fauna (*17*); and (ii) the limited phenotypic data that are used in most analyses of the morphological diversification of placentals. Phenotype is the object of natural selection, as the interface between organisms and their environment, but most studies reduce complex morphologies to highly simplified metrics such as body size (*11*, *12*) or discrete binary characters (*9*, *13*), hindering robust understanding of the influence of social, ecological, and developmental factors on morphological evolution.

Here, we reconstruct the pattern and drivers of the morphological diversification of Placentalia with a quantitative analysis of cranial evolution that samples the full breadth of living and extinct placental mammal diversity. Our dense three-dimensional (3D) morphometric dataset (757 landmarks and sliding semilandmarks) for 322 species spans the Cenozoic Era and represents every extant family and a majority of extinct orders (Figs. 1 and 2, fig. S1, table S1, and data S1). We focus on the cranium because it is a feature-rich structure that performs several critical functions implicated in placental mammal success, from feeding, fighting, and communication to housing and protecting sensory structures and the brain. Given the ongoing debate on the timing of placental mammal diversification and the phylogenetic positions of some extinct clades, we perform these analyses across 1800 evolutionary trees, using multiple topologies and divergence estimates spanning from 100 to 70 million years ago (Ma), and thereby incorporate the impact of this chronological and phylogenetic uncertainty on our understanding of placental mammal evolution. We summarized our results by binning these phylogenetic frameworks into a total of 18 sets, which are divided by tree topology and 5-million–year intervals for the placental mammal root age; for example, 100 trees use tree topology 2 and a divergence estimate for Placentalia ranging between 80 and 85 Ma. With these analyses, we reconstructed the tempo and mode of evolution of the placental mammal skull to robustly test the hypothesis that placental mammals radiated quickly in the aftermath of the K/Pg mass extinction and to assess the primary social, developmental, and ecological factors associated with their morphological diversification.

Results

Cranial variation across placental mammals

Despite the vast ecological range of placental mammals, skull variation is overwhelmingly concentrated into a single region of morphospace, suggesting extensive conservation or convergence of cranial form across all placental mammal superorders (Fig. 1 and fig. S2). There are two other clusters observed, but each is populated by single clades, specifically whales and rodents. The first principal component (PC1) (34.1% of the total variation) is dominated by shifts associated with the land-to-water transition of whales, with two distinct concentrations that represent "terrestrial" and "aquatic" adaptive peaks. Extreme elongation of the premaxilla and maxilla and retraction of the nasals in Cetacea drives change along this axis, with early whales overlapping substantially with terrestrial Laurasian "ungulates" that include Litopterna, Perissodactyla, and Artiodactyla. Several other lineages converge on aspects of this morphology, particularly the retraction of the nasals, including Sirenia, Desmostylia, Proboscidea, and Embrithopoda. The opposite extreme of PC1 is dominated by short-faced, globular euarchontaglirans, particularly Rodentia and Primates. Whales span the full breadth of PC2 (14.9% of the total variation), with the unusual extinct walrus-like whale *Odobenocetops* defining the maximum end of the axis and the early archaeocete *Pakicetus* at the opposite extreme. Many placental mammal lineages are better discriminated along this axis, with extremely dolicocephalic armadillos occupying lower PC2 values and brachycephalic primates, bats, and elephants at the positive end. Rodents are further distinguished on PC3, on which they form a distinct concentration of

[1]Department of Life Sciences, Natural History Museum, London, UK. [2]Department of Genetics, Evolution, and Environment, University College London, London, UK. [3]Department of Vertebrate Zoology, National Museum of Natural History, Smithsonian Institution, Washington, DC, USA. [4]Université Lyon, Université Claude Bernard Lyon 1, CNRS, ENTPE, UMR 5023 LEHNA, Villeurbanne, France. [5]Naturhistorisches Museum Bern, Bern, Switzerland. [6]Institute of Ecology and Evolution, University of Bern, Bern, Switzerland. [7]School of Geography, Earth and Environmental Sciences, University of Birmingham, Birmingham, UK. [8]Department of Biology, University of Wisconsin Oshkosh, Oshkosh, WI, USA. [9]Department of Biology, University of Washington, Seattle, WA, USA. [10]Department of Anatomy, New York Institute of Technology College of Osteopathic Medicine, Old Westbury, New York, NY, USA. [11]Division of Paleontology, American Museum of Natural History, New York, NY, USA. [12]Department of Mammalogy, Division of Vertebrate Zoology, American Museum of Natural History, New York, NY, USA. [13]Department of Paleobiology, National Museum of Natural History, Smithsonian Institution, Washington, DC, USA. [14]Department of Earth and Environmental Sciences, University of Minnesota, Minneapolis, MN, USA. [15]Centre for Integrative Anatomy, Department of Cell and Developmental Biology, University College London, London, UK.
*Corresponding author. Email: a.goswami@nhm.ac.uk

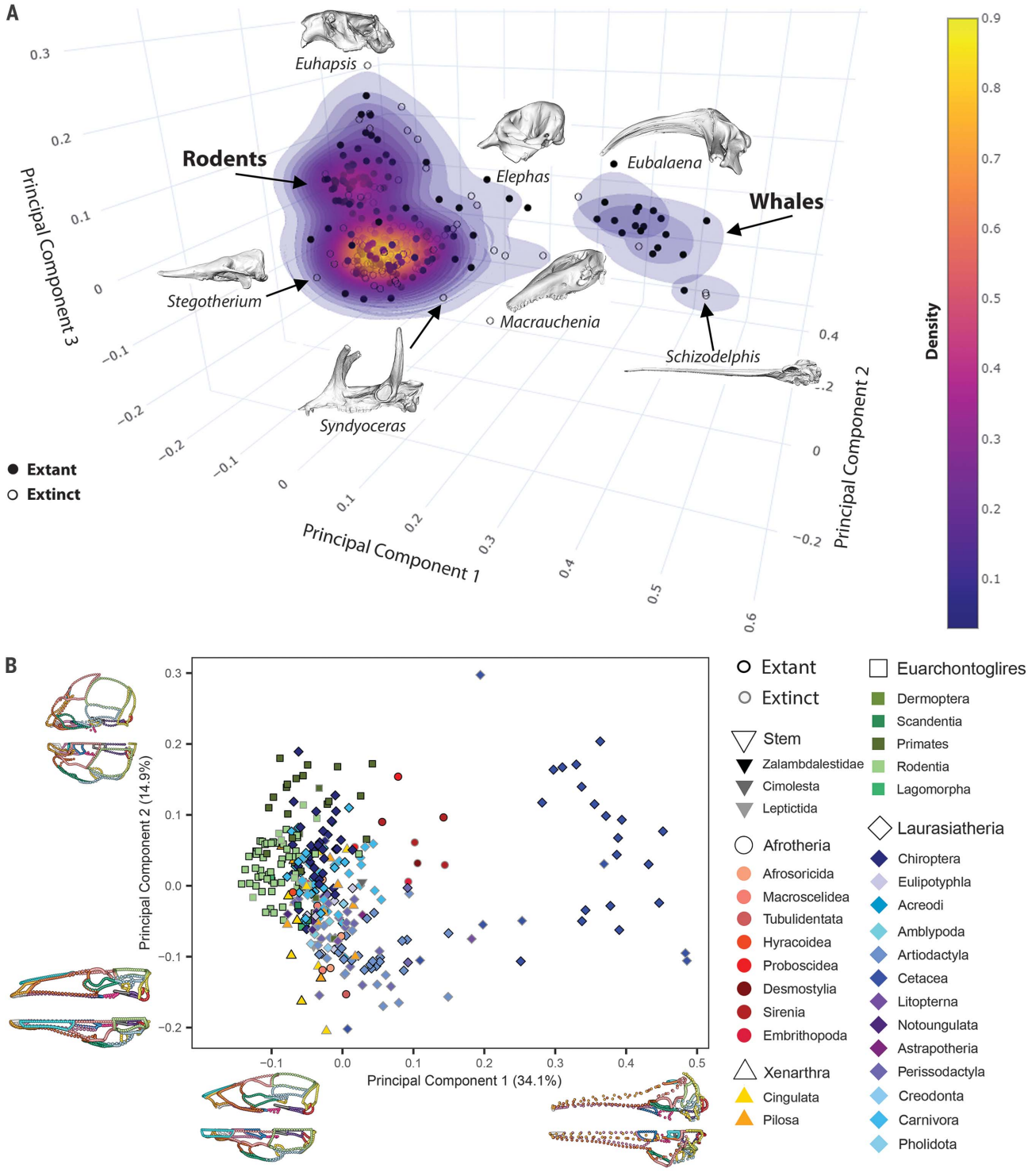

Fig. 1. Cranial variation across placental mammals is highly concentrated. (**A**) Cranial morphospace for placental mammals showing PC1 to 3, with density contours that reflect three concentrations of placental mammal skull shapes (two dominated by single clades) and highlighting specimens along the edges of each of the high-density regions. (**B**) Detailed morphospace of PC1 and 2, showing superordinal and ordinal affiliations of specimens and wireframe models of the variation along each axis. Symbols and colors in the morphospace indicate clade affiliation, as described on the legend (version with color-blind palette provided in fig. S2). Colors on skull wireframes denote different cranial elements (see table S1 for details).

variation that is separate from other terrestrial placental mammals (Fig. 1 and fig. S2) and is driven largely by the height of the facial region, the size of the nasals, and the orientation of the occipital region. Extant and extinct taxa largely overlap in cranial morphospace, with Paleogene to Recent taxa occupying similar positions on the principal axes. Fossil forms fill the gap between the terrestrial and aquatic clusters on PC1, but they also define the extremes of most principal axes, demonstrating the exceptional extinct diversity of placentals. By contrast, the pale fox

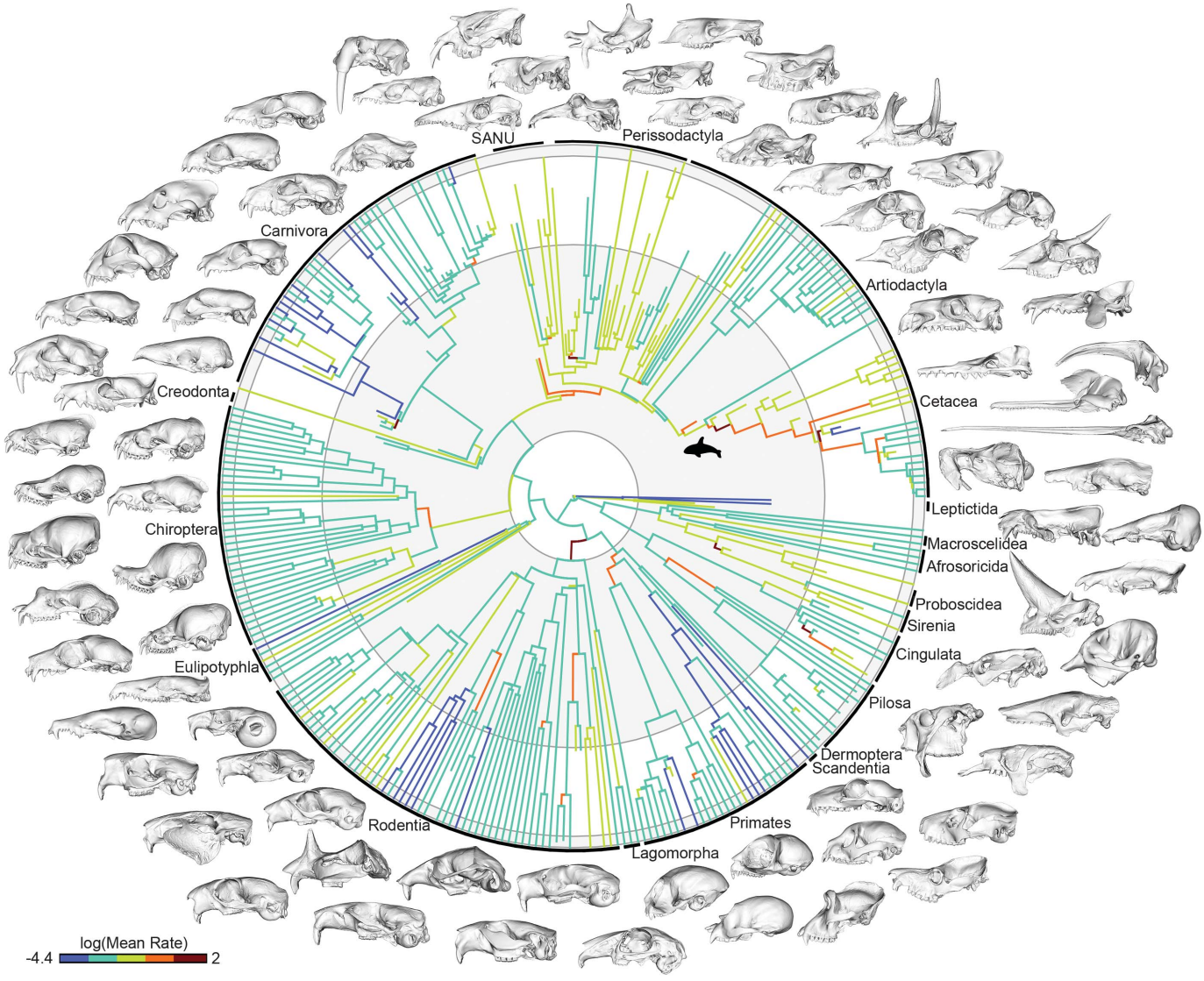

Fig. 2. Rapid evolutionary rates are observed near the base of several placental mammal clades. Estimated branch-specific rates of cranial evolution by using a variable-rates Brownian motion model with a lambda tree transformation, shown here for one example tree (topology 2, root age 80 to 85 Ma, tree 85 of 100). Warmer and cooler colors indicate faster and slower rates of evolution, respectively, with yellow indicating moderate rates. SANU refers to South American native ungulates. Fast branches are concentrated within Cetacea, indicated with a whale icon, as well as more basal branches for several orders. A subset of the sampled skulls is positioned proximal to their terminal branches to demonstrate the immense cranial diversity of living and extinct placentals. Geological age is indicated with alternating shading of circles, from innermost outwards: Cretaceous, Paleogene, Neogene, Quaternary.

(*Vulpes pallida*) is closest to the average cranial shape of extant placental mammals, with an extinct confamilial, the borophagine dog *Desmocyon matthewsi*, possessing a skull most similar to the average shape among the sampled living and extinct mammals.

Tempo of cranial evolution across placental mammals

Bayesian analysis using a reversible-jump Markov chain Monte Carlo (MCMC) algorithm supported variable-rates Brownian motion with a lambda tree transformation (λ = 0.629 to 0.741) as the best supported model of evolution across every phylogenetic topology and divergence time bin sampled in this study (fig. S3). Despite vast differences in the estimated root age for placentals, which ranges from 100 to 70 million years in the phylogenetic hypotheses included here, the results are notably consistent, with little to no difference in positions of rate shifts or relative rates of evolution across the placental mammal tree (Fig. 2 and fig. S4). Rate shifts are clustered at the base of Placentalia, varying slightly in whether they occur at the basal nodes for each superorder or more inclusive nodes (e.g., Boreoeutheria and Atlantogenata) and demonstrating an increase in rate from stem to crown Placentalia (fig. S4). High rates are also concentrated at the base of many orders, reflecting the rapid accumulation of ecological and morphological diversity early in the placental mammal radiation. Multiple rate increases occur along the stem of Cetacea, with particularly fast rates of evolution on the branches leading to fully aquatic whales (basilosaurid archaeocetes plus crown cetaceans), as well as to odontocetes. High rates of evolution are also observed at or near the base of Paenungulata (and/or Sirenia, depending on phylogenetic tree), Cingulata, Primates (and/or Catarrhini), Rodentia, and

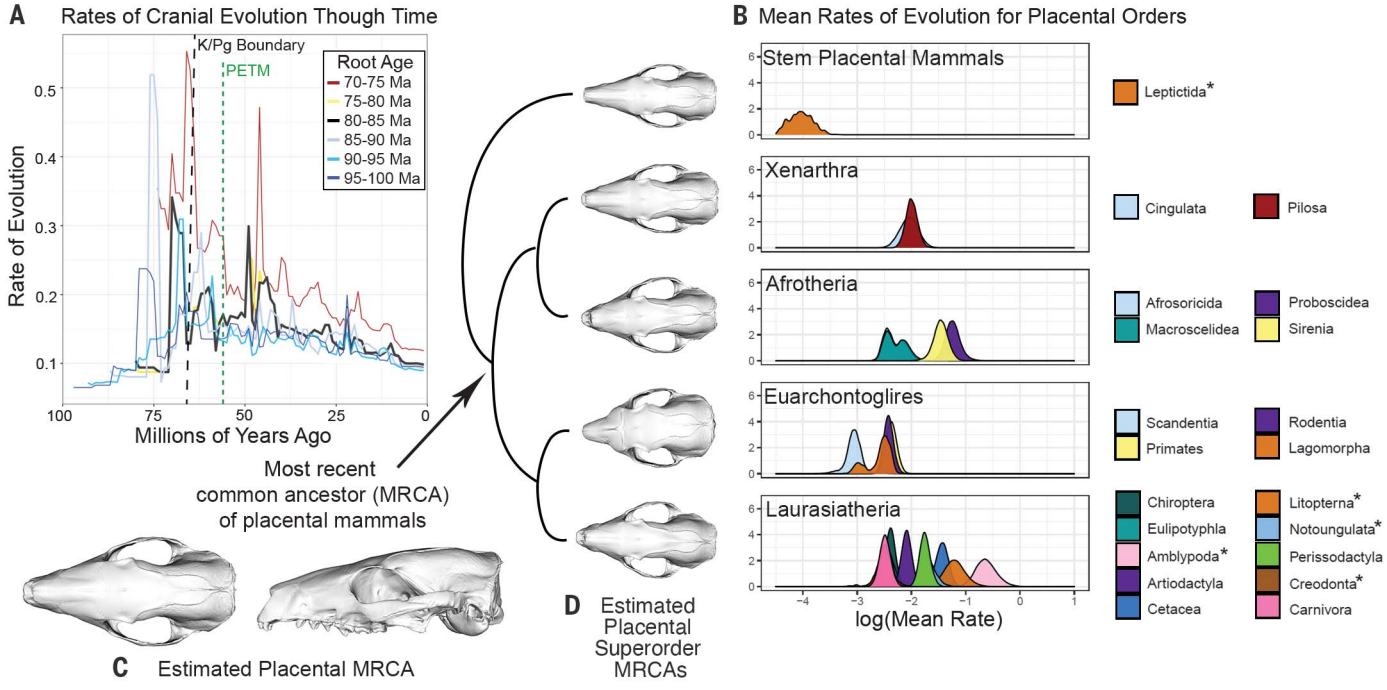

Fig. 3. Rates of evolution peak early in placental mammal evolution and attenuate through time. (**A**) Rates of evolution through time are shown for one sample tree per root age for topology 2, colored by root age, and clade-specific tip rates and ancestral estimates are shown for topology 2, root age 80 to 85, tree 85, as in Fig. 2. The K/Pg boundary and the PETM are indicated with red and green lines, respectively. (**B**) Subsetting terminal branch rates by each order demonstrates the slow pace of evolution in stem placental mammals and euarchontoglirans, in contrast to Afrotheria and several laurasiatherian clades. Asterisk indicates wholly extinct orders. (**C** and **D**) Estimated ancestral cranial shapes (excluding teeth and bullae) for (C) Placentalia and (D) each superorder, by using *Vulpes pallida* for the reference mesh, suggest a marked similarity among the estimated MRCAs for placental mammal superorders.

Chiroptera. There are relatively fewer high rates of evolution observed in less-inclusive clades, but high rates are observed on the branches leading to hominids, saber-toothed cats, pinnipeds, beavers, camels, yangochiropteran bats, and the extinct large-bodied brontothere perissodactyls (Fig. 2 and fig. S4).

Placing evolutionary rates in temporal context necessarily depends heavily on the divergence estimates of the phylogenetic framework. Nonetheless, the distribution of evolutionary rates across a range of phylogenetic hypotheses is strongly indicative that the tempo of cranial evolution increased rapidly early in placental mammal evolution, proximal to the end-Cretaceous mass extinction, and fell equally rapidly, in contrast to studies of body size evolution in extant taxa (*4*, *5*). This initial burst is followed by long-term decline, but this decline is punctuated by multiple smaller peaks throughout the Cenozoic, a pattern that we describe as "attenuated evolution," indicating the decreasing amplitude of peaks in evolutionary rate along a backdrop of declining rates. The initial radiation and declining rates are consistent with an early burst model (*18*), but the presence of numerous intermediate peaks in evolutionary rates distinguishes this pattern from a standard early burst. The declining size of those peaks likely reflects increasingly limited niche space with distance from the K/Pg mass extinction, whereas their timing, allowing for the aforementioned uncertainties, likely reflects subsequent bursts of diversification that are associated with major climatic and geologic events. Several scenarios reconstruct a large peak in rates in the early to middle Eocene and smaller peaks near the Eocene-Oligocene and Oligocene-Miocene boundaries, all of which are associated with transitions between warmer and cooler climates (Fig. 3). By contrast, the impact of the rapid warming event at the Paleocene-Eocene boundary, the Paleocene-Eocene Thermal Maximum (PETM), on evolutionary rates is ambiguous, with sharp declines, small increases, or little change in rate during this interval, depending on the estimated root age of Placentalia.

Both the slowest and the fastest evolving clades in this study are wholly extinct lineages that straddle the end-Cretaceous mass extinction (Fig. 3 and fig. S5). Stem placental mammals with unambiguous Late Cretaceous origins and a rich fossil record evolved much more slowly than all crown placental mammals in every phylogenetic framework. "Archaic" and South American native ungulates (SANU), both of which first appear in the fossil record in the Paleocene in the aftermath of the mass extinction, display the fastest rates of evolution in every scenario. Comparing the overall rates of cranial evolution across orders also demonstrates a clear dissociation of taxonomic diversification and morphological evolution in the crown placental mammal radiation. Irrespective of topology and divergence estimates, laurasiatherian and afrotherian clades display the fastest rates of cranial evolution (Fig. 3 and fig. S5), whereas the most speciose placental mammal orders, Rodentia and Chiroptera, show some of the lowest evolutionary rates for cranial shape. The relative ranking among the five orders with the fastest rates of cranial evolution varies depending on topology and divergence time bin but always includes Cetacea, Proboscidea, Sirenia, and the extinct orders Litopterna and "Amblypoda" (a likely paraphyletic grouping of early Cenozoic large-bodied ungulates). Notably, members of the defunct, paraphyletic "Insectivora," including Afrosoricida, Macroscelidea, Scandentia, and Eulipotyphla, consistently show some of the slowest rates of evolution, which may have contributed to the long-standing difficulties with ascertaining their phylogenetic relationships on the basis of morphology alone.

Among extant superorders, Euarchontoglires is consistently the slowest evolving, with all clades, including rodents and primates, exhibiting some of the slowest evolutionary rates among placentals. The xenarthran clades all consistently

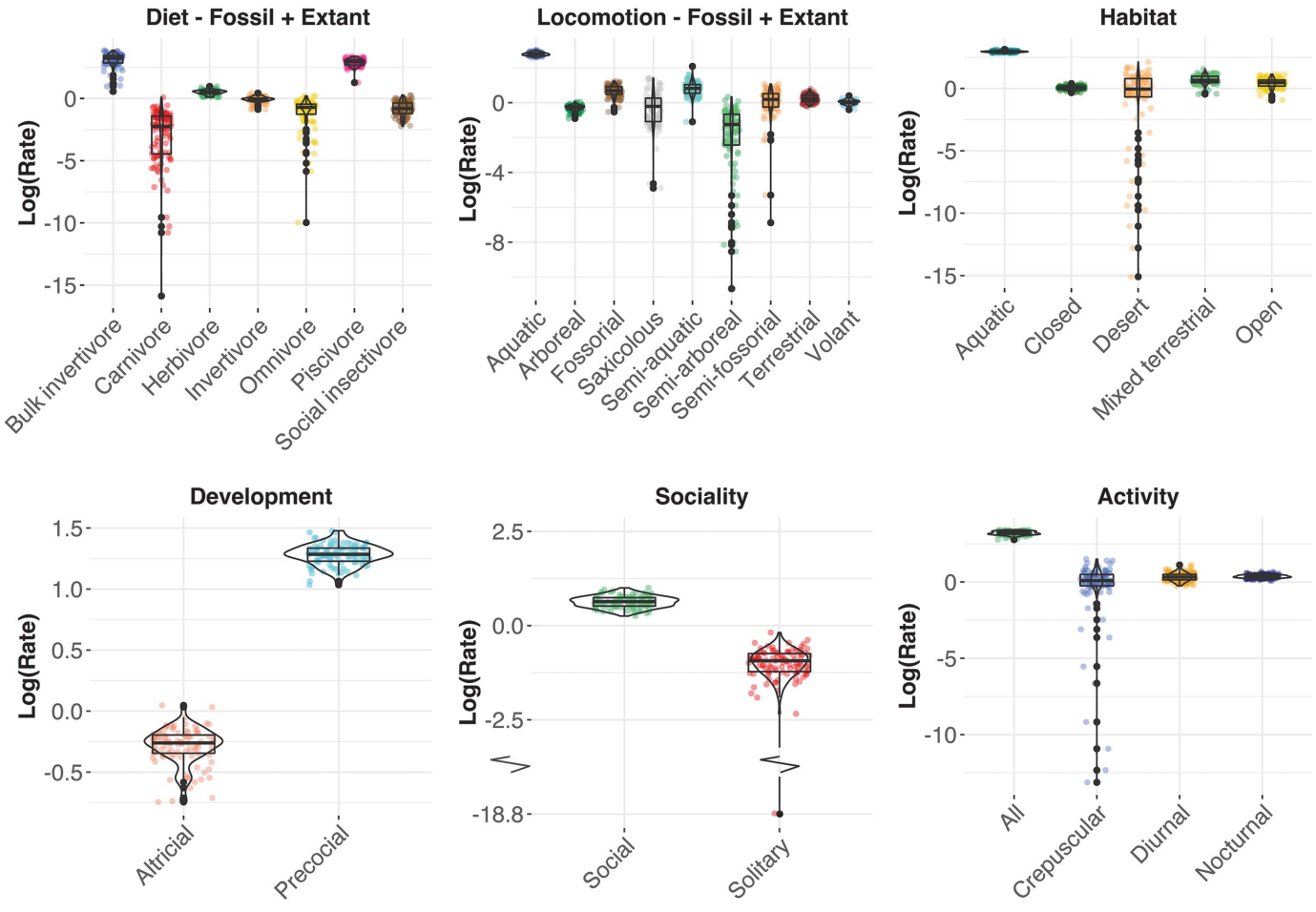

Fig. 4. Aquatic, herbivorous, precocial, and social placental mammals evolve at the fastest rates. Rates of evolution on the basis of ecological and life-history traits for placentals, with diet and locomotion estimated for all living and extinct taxa sampled, whereas the other four categories are limited to extant taxa. Distributions represent results from 100 sampled trees for topology 2, root age 80 to 85.

display an intermediate rate of evolution relative to other placentals, whereas laurasiatherians show the broadest range of evolutionary rates across orders. Other than the fast-evolving aquatic or extinct ungulates and slow-evolving bats noted above, the other laurasiatherians show a division between herbivorous ungulate orders (Artiodactyla, Perissodactyla, and Notoungulata) that evolve at moderate rates, whereas carnivorous laurasiatherians, including Carnivora and the extinct creodonts, display relatively slow rates of evolution. Although we do not quantify taxonomic diversification in this study, our results do suggest that the expected close association of rates of speciation and rates of phenotypic evolution may not extend cleanly to the placental mammal skull. This expectation stems from hypotheses of positive coupling between lineage splitting and adaptation to new niches via phenotypic evolution (*19*). By contrast, numerous examples exist of taxonomic diversification occurring in the absence of ecological or morphological divergence (*20*). Recent study of rates of body size evolution and speciation in several vertebrate clades identified a general relationship between these two rates within each vertebrate class but noted that the strength of this association varied widely in subclades within each class. Moreover, some smaller clades displayed a negative relationship between rate of speciation and that of body size evolution (*20*). Similarly, the lack of a clear association between taxonomic diversity and rate of cranial evolution across placental mammals does not preclude a stronger association existing within placental mammal clades. A focused analysis of this relationship, taking into account the ongoing debate on the ability to accurately estimate rates of taxonomic diversification (*21*), is needed, but it is worth considering whether the likely drivers of nonadaptive radiations, such as geographic isolation, may be more pronounced in smaller taxa, such as those that dominate the two most speciose placental mammal clades, Rodentia and Chiroptera.

Drivers of cranial evolution in placental mammals

We further examined the influences of size, diet, and locomotion on skull shape and rate of cranial evolution using multivariate phylogenetic linear models fitted by penalized likelihood, across the same distribution of phylogenetic tree topologies and divergence time bins that we described above. The additional factors of habitat, development (altricial or precocial), diel activity pattern, and social structure (social or solitary) were further examined for the 207 extant species (data S1). When limited to extant taxa, size and diet were the only factors consistently supported as significantly influencing cranial shape and significantly interacting with each other across all phylogenetic frameworks and time bins ($p < 0.05$; table S2). Locomotion has a significant, albeit weaker, effect on skull shape in all but the youngest divergence time bin (70 to 75 Ma), whereas habitat type was supported as a significant factor in a minority of analyses. Analyses that include extinct taxa are congruent with these results, with diet and size showing the strongest and most consistent influence on cranial shape, as well as having a significant interaction (table S2). Shape changes associated with increased size are concentrated in

the elongation of the rostral region (fig. S6), as suggested by previous studies (*22*). Large size is additionally associated with retraction of the nasals, which is noted in numerous lineages as described above. Variation associated with dietary categories also reflects traits long identified as informative for ecomorphological analyses, including a larger sagittal crest in carnivores, reduced zygomatics in social insectivores, and rostrum elongation and cranial telescoping in bulk invertivores (a category that is composed entirely of cetaceans).

Although most of the factors that we examined are not significantly associated with cranial shape, there are substantial differences in the rate of cranial evolution associated with these factors, which could be informative for modeling species response to environmental change. In particular, diet, locomotion, social structure, and development show significant differences in cranial rate among character states (Fig. 4 and fig. S7). Dietary categories dominated by aquatic taxa, specifically bulk invertivores and piscivores, evolve the fastest, followed by herbivores. Aquatic and semiaquatic mammals evolve the fastest among locomotor categories, with arboreal and semiarboreal showing comparatively slow evolution. Aquatic mammals similarly dominated among habitat categories, whereas desert taxa exhibit a broad range of rates. Notably, social animals evolve significantly faster than solitary animals, which is potentially due to pressure for elaborate cranial ornamentation in many social species. Precocial species also evolve at a markedly faster rate than altricial mammals, suggesting that extended parental care of young may result in overall slower rates of evolution. Placental mammals without a fixed period of activity, a category that is dominated by fast-evolving whales and proboscideans, evolve more rapidly than diurnal, nocturnal, or crepuscular species, but there are no significant differences among taxa that display these latter three activity patterns. Some of these patterns, such as fast rates in bulk invertivores, are clearly driven by cetaceans. However, several of the character states exhibited by some or most cetaceans are shared with other placentals, and these noncetacean taxa also display higher rates of evolution. For example, aquatic mammals in this dataset include cetaceans, pinnipeds, sirenians, and desmostylians, all of which display elevated rates of skull evolution. Other character states associated with higher rates of evolution, such as precociality, sociality, and cathemeral activity pattern, are observed across placentals. In particular, these states are exhibited by many terrestrial herbivores (another fast-evolving ecological group), as well as cetaceans (fig. S8), demonstrating that these results are not solely driven by a single, fast-evolving clade.

Although not considered explicitly here, we may expect postcranial systems to diverge from the patterns observed here, particularly in terms of the differences across clades. Specifically, we may expect higher rates of postcranial evolution in bats and euarchontans, as well as in arboreal and semiarboreal taxa more generally, in contrast to the low rates of cranial evolution that we observed for these groups. More similarity in temporal pattern of cranial and postcranial evolution is likely, because those are likely driven by extrinsic phenomenon, such as mass extinctions or large-scale environmental change. However, some of the most extreme postcranial transitions, which are associated with the appearance of fully aquatic or fully volant mammals, occur during the Eocene. Quantifying postcranial evolution would thus likely increase the amplitude of evolutionary rates during that interval, but further work along these lines is needed to test this hypothesis.

Ancestral estimations of the earliest placental mammals and implications for resolving their origins

We used our extensive sample of living and extinct placental mammals to estimate cranial shapes for the most recent common ancestor (MRCA) of placental mammals and of each of the four placental mammal superorders (Fig. 3). Regardless of the starting 3D mesh used (which is shown here for *V. pallida*, the most average extant placental mammal in this sample), ancestral estimates for the four superorders are very similar, with only the euarchontogliran MRCA distinguished by a broader vault and a shorter and narrower rostrum. Subtle differences among all superordinal MRCAs exist, largely in the breadth and tapering of the rostrum. However, the similarities in these ancestral reconstructions may explain the persistent difficulties with identifying unambiguous Cretaceous crown placentals, despite the near certain divergence of the superorders in advance of the end-Cretaceous mass extinction. Rather than reflecting shortcomings of the fossil record or phylogenetic methodologies, this uncertainty may be due to the lack of clear morphological differences among the earliest representatives of the placental mammal superorders (*7*). This more pernicious source of uncertainty may be unresolvable, but fortunately, our results demonstrate that reconstructions of the tempo and drivers of the exceptional morphological diversification of placental mammals are robust to considerable uncertainty in both phylogenetic topology and the timing of their initial radiation.

Materials and methods

Our dataset samples 322 crown and stem placental mammals, including 207 extant and 115 extinct species. Sixty-six 3D landmarks and 69 semilandmark curves were collected for the left side of the skull by using Stratovan Checkpoint (Stratovan, Davis, CA, USA). Landmarks and semilandmarks were imported into R for analysis, in which curves were resampled to a common number of semilandmarks, slid to minimize bending energy, and registered with generalized Procrustes analysis, which resulted in a total of 757 3D landmarks and sliding semilandmarks. Data on diet, locomotion, habitat, development, social structure, and activity pattern were collected from the published literature.

In the absence of a well-resolved phylogenetic hypothesis that samples all living and extinct taxa in our dataset, we constructed an extensive range of alternative phylogenies. Starting with a set of node-dated trees from the posterior distribution of a recent species-level molecular analysis of placental mammal relationships (*14*), we binned these trees into six 5-million–year bins (70 to 75 Ma, 75 to 80 Ma, 80 to 85 Ma, 85 to 90 Ma, 90 to 95 Ma, and 95 to 100 Ma). We then grafted in fossil taxa on the basis of a suite of recent morphological phylogenetic analyses (see supplementary materials), resulting in three alternative topologies that capture the major points of uncertainty, and generated 419,400 alternative trees to capture uncertainty in divergence estimates. Lastly, we subsampled this set to 1800 trees, 100 for each of the six 5-million–year root-age bins for each of the three topologies, which was used in subsequent analyses.

Macroevolutionary analyses

To examine the overall pattern of cranial variation across placentals, we conducted a principal components analysis using Procrustes-aligned 3D data and reconstructed wireframe models for the minimum and maximum shapes on the primary axes of variation. We further estimated the ancestral shape for the placental MRCA and each superordinal MRCA by maximum likelihood and warping of a reference shape to the ancestral estimates.

We assessed 10 alternative evolutionary models (variable- and single-rate models for Brownian motion [BM], Ornstein-Uhlenbeck, and BM with lambda, kappa, or delta tree transformations) for cranial evolution using phylogenetic PC scores that represented 95% of the total variation in the dataset and a reversible-jump MCMC algorithm implemented in BayesTraits v. 3 (*5*). For the best supported model, we binned rates by geological time and plotted their pattern through time for one randomly selected tree from 18 alternative tree topologies and divergence estimate bins. We further extracted rates for the terminal branches and plotted them by clade to assess differences in mean rate across clades.

We assessed the association of life-history and ecological traits on cranial variation and

evolutionary rates using Type II phylogenetic multivariate analyses of variance (phylogenetic regressions) on the Procrustes coordinates with log centroid size and each of the six factors as predictors across the same 18 trees. We conducted one analysis of size, diet, and locomotion for the full dataset of living and extinct species (n = 322) and a second one of all six factors for just the extant taxa (n = 207). Subsequently, we used a state-specific Brownian motion model to estimate rates of evolution for each ecological and life-history state across the full suite of 1800 trees. Further details of all materials and methods are provided in the supplementary materials.

REFERENCES AND NOTES

1. C. J. Burgin, J. P. Colella, P. L. Kahn, N. S. Upham, *J. Mammal.* **99**, 1–14 (2018).
2. G. G. Simpson, *Biol. Rev. Camb. Philos. Soc.* **12**, 1–46 (1937).
3. N. Cooper, A. Purvis, *Am. Nat.* **175**, 727–738 (2010).
4. J. Clavel, H. Morlon, *Proc. Natl. Acad. Sci. U.S.A.* **114**, 4183–4188 (2017).
5. C. Venditti, A. Meade, M. Pagel, *Nature* **479**, 393–396 (2011).
6. D. M. Grossnickle, E. Newham, *Proc. Biol. Sci.* **283**, 20160256 (2016).
7. N. Brocklehurst, E. Panciroli, G. L. Benevento, R. B. J. Benson, *Curr. Biol.* **31**, 2955–2963.e4 (2021).
8. T. J. D. Halliday, P. Upchurch, A. Goswami, *Proc. Biol. Sci.* **283**, 20153026 (2016).
9. R. M. D. Beck, M. S. Y. Lee, *Proc. Biol. Sci.* **281**, 20141278 (2014).
10. M. S. Springer *et al*., *Mol. Phylogenet. Evol.* **106**, 86–102 (2017).
11. R. W. Meredith *et al*., *Science* **334**, 521–524 (2011).
12. S. Álvarez-Carretero *et al*., *Nature* **602**, 263–267 (2022).
13. M. A. O'Leary *et al*., *Science* **339**, 662–667 (2013).
14. T. J. D. Halliday *et al*., *Proc. Biol. Sci.* **286**, 20182418 (2019).
15. N. S. Upham, J. A. Esselstyn, W. Jetz, *PLOS Biol.* **17**, e3000494 (2019).
16. N. M. Foley, M. S. Springer, E. C. Teeling, *Philos. Trans. R. Soc. Lond. B Biol. Sci.* **371**, 20150140 (2016).
17. T. R. Lyson *et al*., *Science* **366**, 977–983 (2019).
18. L. J. Harmon *et al*., *Evolution* **64**, 2385–2396 (2010).
19. G. G. Simpson, *The Major Features of Evolution* (Columbia Univ. Press, 1953).
20. C. R. Cooney, G. H. Thomas, *Nat. Ecol. Evol.* **5**, 101–110 (2021).
21. S. Louca, M. W. Pennell, *Nature* **580**, 502–505 (2020).
22. A. Cardini, P. D. Polly, *Nat. Commun.* **4**, 2458 (2013).

ACKNOWLEDGMENTS

We are indebted to the numerous colleagues, curators, and collections staff at international museums that provided access to specimens for this project, in particular R. Portela Miguez, R. Pappa, P. Brewer, R. Sabin, and L. Tomsett (NHM); P.-H. Fabre (Université de Montpellier); J. Galkin, R. O'Leary, and A. Gishlick (AMNH); G. Rößner (BSP); S. and R. Boessenecker (CCNHM); B. Simpson (FMNH); D. Miao (KU); J. Chupasko (MCZ); S. McLeod, X. Wang, and J. Velez-Juarbe (LACM); J. Ashby and P. Viscardi (LDUCZ); M. Reguero (MLP); G. Billet, J. Cuisin, and G. Veron (MNHN); P. Holroyd, M. Goodwin, and J. Tseng (UCMP); B. Sanders (UMMP); A. Millhouse and S. Peurach (USNM); C. Norris and D. Brinkman (YPM); R. Secord and G. Carter (UNSM); and L. Costeur (NMB). We are grateful to V. Fernandez and B. Clark (NHM) and J. Keller (UMN) for support in microCT scanning and to the "plate-forme de morphometrie" of the UMS 2700 (CNRS, MNHN) for access to the surface scanner. We thank E. Watt (NHM/UCL) for uploading scans to online repositories. We are grateful to the two anonymous reviewers and the editor for their thoughtful comments. We thank V. Herridge for putting a name to this phenomenon.

Funding: European Research Council grant STG-2014-637171 (to A.G.), National Science Foundation SF-EAR 1349607 (to J.H.G., B.L.B., A.G., and M.C.), Gerstner Scholar Postdoctoral Research Fellowship (to A.C. and N.B.S.), Natural Environment Research Council Doctoral Training Partnership training grant NE/L002485/1 (to E.J.C.), Horizon 2020 MCSA Fellowship IF 797373-EVOTOOLS (to J.C.), National Science Foundation EAR 1338262 (to D.L.F.), and Labex BCDiv 10-LABX-0003 (to A.C.F.). **Author contributions:** Conceptualization: A.G.; Methodology: A.G., R.N.F., J.C., A.C.F., and A.W.; Software: A.G., R.N.F., J.C., A.W., and A.C.F.; Investigation: A.G., R.N.F., E.N., J.C., E.J.C., A.C.F., T.J.D.H., A.C., M.C., B.L.B., J.H.G., N.B.S., and D.L.F.; Visualization: A.G. and R.N.F.; Funding acquisition: A.G., E.C., J.H.G., B.L.B., A.C., and N.B.S.; Writing—original draft: A.G.; Writing—review and editing: A.G., R.N.F., E.N., J.C., E.J.C., A.C.F., T.J.D.H., A.C., M.C., B.L.B., J.H.G., N.B.S., D.L.F., and A.W. **Competing interests:** The authors declare that they have no competing interests. **Data and materials availability:** Morphometric data and novel code are provided on Github (https://github.com/anjgoswami/Goswami_et_al_Placental_evolution_2022). 3D meshes for all specimens are available for free download on phenome10k.org or morphosource.org, as detailed in data S1, unless specifically restricted by specimen repositories. All specimen and species details, including physical and online repository information and trait data, are provided in data S1.

SUPPLEMENTARY MATERIALS

science.org/doi/10.1126/science.abm7525
Materials and Methods
Figs. S1 to S8
Tables S1 and S2
References (*23*–*97*)
Data S1

Submitted 8 October 2021; accepted 20 September 2022
10.1126/science.abm7525

Science

Attenuated evolution of mammals through the Cenozoic

Anjali GoswamiEve NoiraultEllen J. CoombsJulien ClavelAnne-Claire FabreThomas J. D. HallidayMorgan ChurchillAbigail CurtisAkinobu WatanabeNancy B. SimmonsBrian L. BeattyJonathan H. GeislerDavid L. FoxRyan N. Felice

Science, 378 (6618), • DOI: 10.1126/science.abm7525

Becoming diverse

Mammals have the greatest degree of morphological variation among vertebrate classes, ranging from giant whales to the tiny bumblebee bat. How they evolved this level of variation has been a persistent question, with much debate being centered around the timing and tempo of evolutionary change. Goswami *et al*. looked across a large dataset of extinct and extant mammalian skulls and found that the rate of evolutionary change peaked around the time of the Cretaceous-Paleogene boundary and has general tapered off since then (see the Perspective by Santana and Grossnickle). Certain lifestyles, such as aquatic habitats or herbivory, led to faster change, whereas in some species such as rodents, morphological change appeared to be decoupled from taxonomic diversification. —SNV

Science (ISSN) is published by the American Association for the Advancement of Science. 1200 New York Avenue NW, Washington, DC 20005. The title *Science* is a registered trademark of AAAS.